

# Dynamical bistability in the driven circuit QED

V. Peano<sup>1,3</sup> and M. Thorwart<sup>2,3</sup>

<sup>1</sup> *Physikalisches Institut, Universität Freiburg, 79104 Freiburg, Germany*

<sup>2</sup> *Freiburg Institute for Advanced Studies (FRIAS), Universität Freiburg, 79104 Freiburg, Germany*

<sup>3</sup> *Institut für Theoretische Physik, Heinrich-Heine-Universität Düsseldorf, 40225 Düsseldorf, Germany*

(Dated: December 27, 2018)

We show that the nonlinear response of a driven circuit quantum electrodynamics setup displays antiresonant multiphoton transitions, as recently observed in a transmon qubit device. By including photon leaking, we explain the lineshape by a perturbative and a semiclassical analysis. We derive a bistable semiclassical quasienergy surface whose groundstate is squeezed, allowing for a squeezing-dependent local effective temperature. We study the escape dynamics out of the metastable state and find signatures of dynamical tunneling, similar as for the quantum Duffing oscillator.

PACS numbers: 78.47.-p, 74.50.+r, 42.50.Pq, 42.50.Hz

One of the nontrivial fundamental models of quantum physics is the Jaynes-Cummings (JC) model [1]. It was introduced to describe the interaction of a two-level atom and a single quantized electromagnetic field mode. Being sufficiently simple, its dynamics is very rich though, including Rabi oscillations, collapse and revival phenomena, squeezing, entanglement, Schrödinger cat and Fock states, and photon antibunching [2]. Beyond quantum optical set-ups, it is applicable to many situations of nanocircuit quantum electrodynamics (QED), such as Cooper pair boxes [3], superconducting flux qubits [4], Josephson junctions [5], and semiconductor quantum dots [6]. In particular, the latter setups allow to explore the regime of strong coupling and nonlinear response.

Recently, unique nonlinear features have been detected in the transmitted heterodyne signal of a superconducting transmon qubit device [7]. For weak driving, the two well-known vacuum Rabi resonances reflect transitions between the groundstate and the first/the second excited state of the undriven JC spectrum. Their difference in energy is  $2\hbar g$ , where  $g$  is the interaction strength of the qubit and the harmonic mode. For increasing driving, each vacuum Rabi peak supersplits into additional (anti-)resonances with the characteristic  $\sqrt{n}$  spacing. The measurements have been corroborated with accurate numerical simulations [7].

In this Letter, we provide a complete physical picture for the dissipative dynamics of the Purcell-limited nonlinear response of the driven JC model in terms of quantum multiphoton (anti-)resonances. The underlying physical mechanism is revealed by perturbative arguments in the rotating frame in presence of photon leaking. The lineshape is determined by the ratio of the Rabi frequency and the dissipation strength, allowing for a direct experimental control. Beyond the perturbative regime, we derive a semiclassical quasienergy surface which is bistable. Its groundstate is an amplitude squeezed state and displays large out-of-phase oscillations. It is significantly populated at a multiphoton (anti)resonance, and is metastable away from resonance. The dissipative dynamics at zero temperature involves quantum activation [8, 9], but also shows dynamic resonant tunneling [10].

Furthermore, we reveal deep analogies with the quantum Duffing oscillator [10, 11, 12, 13].

We start from a harmonic oscillator with frequency  $\omega_r$  which is coupled with strength  $g$  to a qubit and which is driven with frequency  $\omega_{\text{ex}}$  and field strength  $f$ . In the frame rotating with  $\omega_{\text{ex}}$  and for  $\delta\omega \equiv \omega_r - \omega_{\text{ex}}, g, f \ll \omega_r$ , we perform a rotating-wave approximation and obtain the Hamiltonian of the driven JC model ( $\hbar = k_B = 1$ )

$$H_{\text{JC}} = \delta\omega \left( a^\dagger a + \frac{\sigma_z}{2} \right) + \frac{g}{2} (a^\dagger \sigma_- + a \sigma_+) + \frac{f}{2} (a^\dagger + a), \quad (1)$$

with  $\sigma_\pm = \sigma_x \pm i\sigma_y$ . Here,  $\sigma_j$  are the Pauli matrices. The undriven JC model has the quasienergies  $\varepsilon_0 = -\delta\omega/2$ ,  $\varepsilon_{n,\pm} = (n-1/2)\delta\omega \pm g\sqrt{n}$  and the quasienergy states  $|\phi_0\rangle = |0, g\rangle$ ,  $|\phi_{n\pm}\rangle = (|n-1, e\rangle \pm |n, g\rangle)/\sqrt{2}$ . We will refer to latter as  $n$ -photon (dressed) states with two spin directions  $\pm$ . For  $f \neq 0$ , avoided crossings of the quasienergy levels arise, which correspond to  $N$ -photon transitions at  $\delta\omega = \pm g/\sqrt{N}$ . To have well separated resonances, we consider the regime  $g \gg f$ . Around the resonance, the zero-photon state  $|\phi_0\rangle$  and the  $N$ -photon dressed state  $|\phi_{N\pm}\rangle$  display Rabi oscillations with the Rabi frequency  $\Omega_N \propto f^N/g^{N-1}$ .

Due to the suppression of  $1/f$ -noise, transmon qubits are Purcell-limited in the resonant regime considered here [14]. For low temperatures  $T \ll \omega_{\text{ex}}$ , we incorporate Purcell dissipation by means of the simple Lindblad master equation for the density operator

$$\dot{\rho} = -i[H, \rho] + \frac{\kappa}{2} ([a\rho, a^\dagger] + [a, \rho a^\dagger]). \quad (2)$$

Then, only photon leaking from the system into the bath is possible. Hence, in absence of multiphoton transitions,  $|\phi_0\rangle$  is dominantly populated in the stationary state. In contrast, at a multiphoton resonance, the stationary state is generated by coherent driving to the  $N$ -photon state and a subsequent relaxation via all the intermediate  $n$ -photon states ( $n \leq N$ ) to the 0-photon state due to photon leaking. Eventually, this nontrivial interplay generates a stationary mixture of all  $n$ -photon states.

We are interested in the nonlinear response characterized by the steady-state intracavity field  $\langle a \rangle = \text{tr}(\rho a) =$

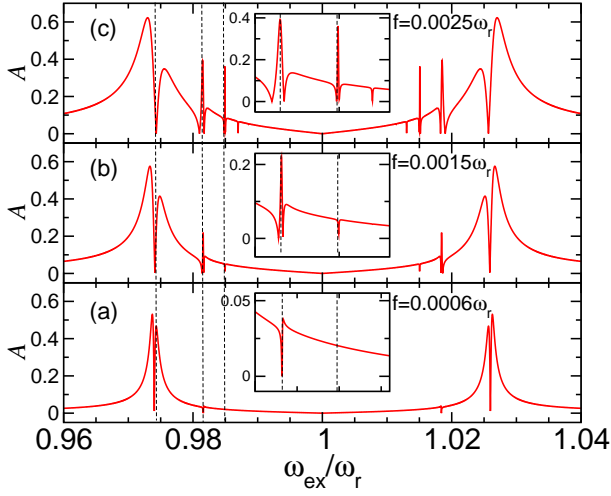


FIG. 1: Amplitude  $A$  as a function of the driving frequency  $\omega_{ex}$  for  $f = 0.0006\omega_r$  (a),  $f = 0.0015\omega_r$  (b) and  $f = 0.0025\omega_r$  (c). Insets: zooms to the corresponding (anti-)resonances marked by the dashed lines. Moreover,  $g = 0.026\omega_r$ ,  $\kappa = 5 \times 10^{-5}\omega_r$ . A realistic value for  $\omega_r/(2\pi)$  is 7 GHz [7, 14].

$Ae^{i\varphi} = \sum_{\alpha\beta} \varrho_{\alpha\beta} a_{\beta\alpha}$ . We discuss the case  $\delta\omega > 0$ , the opposite follows from  $|\phi_{n\pm}\rangle \rightarrow |\phi_{n\mp}\rangle$ ,  $f \rightarrow -f$  and  $\varphi \rightarrow -\varphi + \pi$ . The modulus  $A$  is related to the transmitted amplitude  $A_{tr} \propto A$  and intensity  $I_{tr} \propto A^2$  of the microwave input signal at frequency  $\omega_{ex}$  [7]. In the rotating frame,  $\langle a \rangle < 0$  ( $\varphi = \pi$ ) corresponds to an oscillation out of phase with respect to the drive.

The nonlinear response, in the first instance obtained from a numerical solution, is shown in Fig. 1 for the parameters in the regime of Ref. [7]. The drive induces a splitting of the vacuum Rabi resonance and produces two families of peaks which are symmetric with respect to  $\omega_{ex} = \omega_r$  and which are associated to the  $\pm$  quasienergy states. In each family, (anti)resonances occur which correspond to multiphoton transitions and which are associated to the avoided crossings of quasienergy levels, see Fig. 2c. We note that no antiresonances occur in the photon number  $\langle a^\dagger a \rangle$  [15].

For weak driving (Fig. 1a), only the 1-photon antiresonance is well pronounced. It can be described [7, 13] by a model involving the 0- and the 1-photon state. At resonance, they are equally populated and oscillate with opposite phase yielding zero response. Slightly away from resonance, one of the two states is more populated and a finite response arises. Far away from the resonance, the response again approaches zero. Overall, the lineshape of an antiresonance arises. The antiresonance around  $\omega_{ex} \approx 0.98\omega_r$  corresponds to a 2-photon process (Fig. 1a). This feature also follows from a two state description. The shape is different from the 1-photon antiresonance, due to the background contribution of nonresonant 1-photon mixing processes [11].

For increasing driving, unexpected features arise. The multiphoton antiresonances turn into resonances, see Fig.

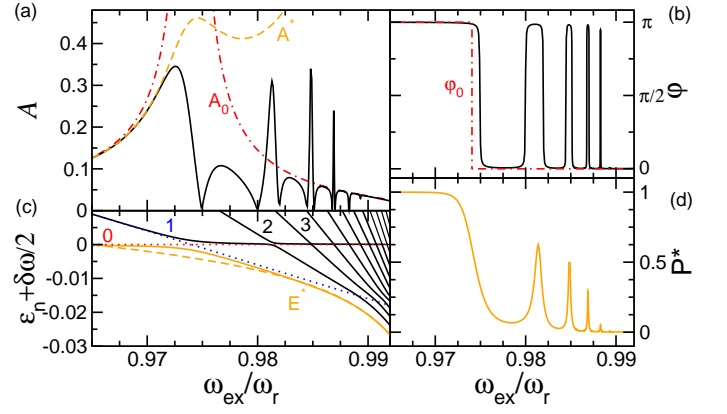


FIG. 2: Nonlinear response of the driven JC model: (a) amplitude, (b) phase, (c) quasienergies, and (d) population of the lowest quasienergy state  $|\psi^*\rangle$  for  $g = 0.026\omega_r$ ,  $f = 0.004\omega_r$ ,  $\kappa = 10^{-4}\omega_r$ . Dashed-dotted red line in (a,b): lowest-order result for non-resonant approximation. Dashed orange line in (a):  $A^* = |\langle \psi^* | a | \psi^* \rangle|$ ; and in (c): semiclassical result Eq. (5) for the lowest quasienergy  $E^*$ .

1b and c. Associated to the behavior of  $A$  are jumps in the phase  $\varphi$ , see Fig. 2b. This already suggests that two quasienergy states - one oscillating in and one out of phase - are alternately populated. Interestingly, the population (Fig. 2d) of the state  $|\psi^*\rangle$  with lowest quasienergy shows peaks at the resonance frequencies. In fact, as we will show below,  $|\psi^*\rangle$  is localized in the bottom of a well of a bistable quasienergy surface.  $|\psi^*\rangle$  is metastable since the bath induces transitions to higher quasienergies states and an escape is always possible, even at zero temperature. This feature has also been reported for the quantum Duffing oscillator [10, 12, 13].

These observations are further substantiated by perturbative arguments. Out of resonance,  $\rho_{00} \simeq 1$  yielding  $\langle a \rangle \simeq -f[(\delta\omega + g)^{-1} + (\delta\omega - g)^{-1}]/4$  up to first order in  $f$ . As follows from Figs. 2 a) and b) (dashed-dotted red lines), the lowest order response  $A_0$  coincides with the exact one away from resonance. Moreover,  $\varphi_0 = \pi$  for  $\delta\omega \leq g$  and  $\varphi_0 = 0$  for  $\delta\omega > g$ .

At the  $N$ -photon-resonance, the system tunnels from  $|\phi_0\rangle$  to  $|\phi_{N-}\rangle$  with probability  $\Omega_N$  and the bath induces decays from  $|\phi_{n-}\rangle$  to  $|\phi_{n-1-}\rangle$  along the ladder  $N \rightarrow N-1 \rightarrow \dots \rightarrow 1 \rightarrow 0$ . The decay rates (in secular approximation) are  $\mathcal{L}_{n-, (n-1)-} = (\sqrt{n} + \sqrt{n-1})^2 \kappa/4$  for  $n \neq 1$  and  $\mathcal{L}_{1-, 0} = \kappa/2$ . Hence, the rate from the 1-photon to the 0-photon state is smallest. Note that the probability of a decay to a state with opposite dressed spin is small, i.e.,  $\mathcal{L}_{(n-1)-, n+}/\mathcal{L}_{(n-1)+, n+} \simeq 1/[16n(n-1/2)]$ . Hence, the population of the 1-photon state is always larger than those of the  $n$ -photon states. In addition, depending on the ratio  $\kappa/\Omega_N$ , qualitatively different stationary populations arise from a competition between tunneling from  $|\phi_0\rangle$  to the top of the ladder,  $|\phi_{N-}\rangle$ , and relaxation down the ladder. For  $\kappa \gg \Omega_N$ , the population of  $|\phi_0\rangle$  is  $\simeq 1$ , because damping is more efficient than

tunneling. Dissipation then completely washes out the resonance, and the response is the same as that off resonance and thus is in phase with the drive. For  $\kappa \simeq \Omega_N$ , a small population  $\rho_{11}$  emerges, contributing  $\rho_{11}a_{11}$  with  $a_{11} = \frac{f}{2(\varepsilon_{1-} - \varepsilon_{2-})} \frac{3+2\sqrt{2}}{4} + \frac{f}{4(\varepsilon_{1-} - \varepsilon_0)} < 0$  since, in the perturbative regime and for  $N < 6$ ,  $\varepsilon_{1-} < \varepsilon_{2-}, \varepsilon_0$ . This leads to a reduced response, forming an antiresonance, see, e.g., the 2-photon antiresonance shown in Fig. 1a. For  $\kappa \ll \Omega_N$ , tunneling is faster than relaxation and the population of  $|\phi_{1-}\rangle$  becomes the largest. Then, the contribution  $\rho_{11}a_{11} < 0$  dominates, leading to an out-of-phase oscillation. For the 2-photon resonance of Fig. 1,  $\kappa/\Omega_2 = \kappa f^2/(\sqrt{2}g) = 2.6$  (a), 0.42 (b) and 0.15 (c).

For increasing driving, the response is qualitatively similar, although the perturbative approach becomes inadequate. In fact, as shown in Fig. 2d, at resonance, there is a large population  $P^*$  of the lowest quasienergy state  $|\psi^*\rangle$ . As follows from Fig. 2c,  $|\psi^*\rangle \neq |\phi_{1-}\rangle$ . In order to account for the importance of  $|\psi^*\rangle$ , we perform next a semiclassical analysis. We switch to the dressed atom picture, by means of the unitary transformation  $R = \exp(\frac{-\pi}{8\sqrt{a^\dagger a + \sigma_z/2 + 1/2}}[a^\dagger \sigma_- - a \sigma_+])$  mapping the JC eigenstates into product states  $|n\sigma\rangle$  (with  $\sigma = g, e$ ). Under this transformation, the undriven JC Hamiltonian becomes diagonal in the spin degrees of freedom

$$\tilde{H} = |\delta\omega| \left( a^\dagger a + \frac{\sigma_z}{2} \right) + g\sigma_z \sqrt{a^\dagger a + \frac{1}{2} + \frac{\sigma_z}{2}} \quad (3)$$

while  $\tilde{a} = R^\dagger a R = a - a \frac{1}{4(a^\dagger a + 1/2)}(1 + \sigma_x) + \mathcal{O}(n^{-3/2})$ . Hence, as expected, the driving as well as the bath-induced relaxation induce spin flip transitions between dressed states. Next, we introduce the canonical variables  $\mathcal{X} = \sqrt{\lambda/2}(a^\dagger + a)$  and  $\mathcal{P} = i\sqrt{\lambda/2}(a^\dagger - a)$ , where  $\lambda = |\delta\omega|/g$  is a dimensionless parameter playing the role of  $\hbar$ . Eventually, neglecting (dressed) spin flips and all other higher order terms, we obtain the transformed Hamiltonian  $\tilde{H} \simeq gQ(\mathcal{X}, \mathcal{P})$  with

$$Q(\mathcal{X}, \mathcal{P}) = \frac{\mathcal{X}^2}{2} + \frac{\mathcal{P}^2}{2} + \frac{\sigma_z}{\sqrt{\lambda}} \sqrt{\frac{\mathcal{X}^2}{2} + \frac{\mathcal{P}^2}{2}} + \frac{f}{g\sqrt{2\lambda}} \mathcal{X}. \quad (4)$$

It can be interpreted as a quasienergy surface in phase space, see Fig. 3a for the qubit groundstate ( $\sigma_z = -1$ ). The corresponding quasiclassical orbits encircle the inner maximum on an external and an internal domain. In addition, there is a range of quasienergies where two orbits are degenerate and a dynamical bistability occurs. The surface for  $\sigma_z = +1$  is a less interesting monotonous function (not shown). The drive induces a tilt generating one stable orbit close to the quasienergy minimum. The orbits near the inner maximum correspond to small photon numbers and are not accurately described by the semiclassical approach.

Let us next consider the dynamics around the minimum at  $\mathcal{P}_{\min} = 0$  and  $\mathcal{X}_{\min} = -(f/g + 1)/\sqrt{2\lambda}$ . A harmonic expansion yields the lowest quasienergy  $E^* =$

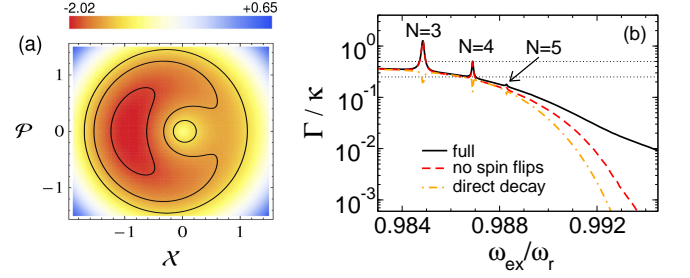


FIG. 3: (a): Quasienergy surface  $Q(\mathcal{X}, \mathcal{P})$  for  $g = 0.026\omega_r$ ,  $f = 0.004\omega_r$ ,  $\kappa = 10^{-4}\omega_r$  and  $\delta\omega = 0.01\omega_r$  ( $T_{\text{eff}} = 0.65$ ). (b) Solid line: Smallest eigenvalue of the Lindblad master equation. Dashed red line: the same without dissipative spin flips. Dashed-dotted orange line: decay rate for  $|\psi^*\rangle \rightarrow |\phi_0^f\rangle$ . Dotted lines correspond to  $\kappa/2$  and  $\kappa/4$ .

$g[Q(\mathcal{X}_{\min}, 0) + (\lambda/2)\omega^*]$  in the semiclassical limit as

$$E^* = -\frac{g}{4\lambda} \left( \frac{f}{g} + 1 \right)^2 + \frac{g}{2} \lambda \sqrt{\frac{f}{g+f}}, \quad (5)$$

with the effective frequency  $\omega^* = \sqrt{f/(g+f)}$ . This result is correct up to  $\mathcal{O}(\lambda^2)$  and is shown in Fig. 2c as orange dashed line. It almost coincides with the exact result, even for small photon numbers  $N = 1$ .

Up to leading order in  $\lambda$ , the groundstate

$$|\psi^*\rangle = R^{-1} D(\mathcal{X}_{\min}) S(r) |0g\rangle \quad (6)$$

is obtained by applying to the vacuum: i) the squeezing operator  $S(r) = \exp[r(a^2 - a^{\dagger 2})/2]$  with squeeze factor  $r = -(\ln \omega^*)/2 = \ln[1 + g/f]/4$ , ii) the translation  $D(\mathcal{X}_{\min}) = \exp[i\mathcal{P}\mathcal{X}_{\min}/\lambda]$  to the minimum, and iii)  $R^{-1}$  to return to the bare atom picture. With this, one can compute the Fock-state representation [16] and all expectation values at leading order. It turns out that  $|\psi^*\rangle$  has sub-Poissonian statistics and shows photon antibunching. This is not surprising, in fact  $D(\mathcal{X}_{\min}) S(r) |0g\rangle$  is an amplitude squeezed state for  $r > 0$ .

Next, we consider the dissipative semiclassical dynamics. As will be shown below, a separation of time scales exists which defines a fast intrawell and a slow interwell relaxation. Deep in the semiclassical limit, the quasienergy states, localized close to the minimum of one well, can be obtained as  $|\psi_n^*\rangle = R^{-1} b^{\dagger n} R |\psi^*\rangle / \sqrt{n!}$  with  $b = a \cosh r + a^\dagger \sinh r - e^r \mathcal{X}_{\min} / \sqrt{2\lambda}$ . In this limit, dissipative transitions occur only between nearest neighbors, with the rates  $\mathcal{L}_{n-1,n} = \kappa n \cosh^2 r$ ,  $\mathcal{L}_{n,n-1} = \kappa n \sinh^2 r$ . Here, the detailed balance condition is fulfilled. When the system is initially in a state with a large photon number, it has a large probability to fall in the basin of attraction of the quasipotential minimum (intrawell relaxation). When also  $\kappa \ll g\lambda\omega^*$ , detailed balance determines an effective Boltzmann distribution  $P_n^* = P^* e^{-n\beta_{\text{eff}}}$ , with effective inverse temperature  $\beta_{\text{eff}} = 2 \ln \coth r$ . We emphasize that this link be-

tween effective temperature and squeezing can be generalized to any driven quantum system with a smooth quasienergy surface and coupled linearly to a bath (e.g., the Duffing oscillator [10, 11, 12, 13] or the parametrically driven oscillator [9]). It can be easily generalized to finite temperatures  $T > 0$  as well. It turns out that the zero temperature limit applies when  $\sinh^2 r$  is much larger than the bosonic occupation number  $\bar{n}(\omega_{\text{ex}}/T)$  of the bath at  $\omega_{\text{ex}}$ . In the opposite limit,  $\beta_{\text{eff}} = \omega_{\text{ex}}/T$ . Since we include here only photon leaking, i.e.,  $\omega_{\text{ex}} \gg T$ , the effective temperature is still small.

On the large time scale, the system decays to the 0-photon state with a rate  $k_-$  (interwell relaxation). From there, it can return to the basin of attraction of the minimum by a driving induced transition with a rate  $k_+$ . The stationary populations of the intrawell states (oscillating out of phase) and the 0-photon state (in phase) are determined by the ratio  $k_-/k_+$ . Off resonance, photon leaking favors the 0-photon state and  $k_- \gg k_+$ . Approaching a resonance,  $k_+$  can increase up to  $\Omega_N/\pi$  and can become comparable to  $k_-$ . Then, the response is qualitatively modified. The resonant-antiresonant transition is governed by the ratio  $k_-/\Omega_N$ .

In the semiclassical regime, the smallest finite eigenvalue  $\Gamma$  of the Lindblad master equation consists of the sum of  $k_+$  and  $k_-$  and is shown in Fig. 3b. The peaks are due to resonant tunneling from the 0- to  $N$ -photon state, whereas off resonance,  $\Gamma \approx k_-$ . There are three mechanisms of decay from the metastable well: (i) The system can decay directly to the 0-photon state with the rate shown in Fig. 3b, dashed-dotted orange line. (ii) The system can climb up the quasienergy well by quantum activation [8]. Both associated rates are expected to decrease exponentially, following  $\propto e^{-c_i/\delta\omega^2}$ , with some constants  $c_i$  (the prefactor varies smoothly with  $\delta\omega$ ), which defines the separation of time scales. (iii) For very small detuning, the escape occurs via bath-induced spin flips. In fact, this mechanism is suppressed only as a power-law  $\Gamma \propto \delta\omega^2$ . To separate (ii) from (iii), we show  $\Gamma$  without the bath-induced spin flips in Fig. 3b (dashed red line), illustrating that spin flips are dominant when the separation of time scales is well defined. Since only a few

states close to the bottom are populated, our solution is stable against a small dephasing of the oscillator [9] or an intrinsic spin relaxation that violates detailed balance. The induced spin-flip rate would be small and remain finite for  $\lambda \rightarrow 0$ , imposing an upper limit to the lifetime of  $|\psi^*\rangle$ . We note that the real parts of the two eigenvalues corresponding to the dissipative and decoherence transition of  $|\phi_{1+}\rangle \rightarrow |\phi_0\rangle$  are not included. They are approximately given by  $\kappa/2$  and  $\kappa/4$ .

Our analysis can be easily extended to any driven nonlinear oscillator coupled bilinearly to a thermal bath. For example, the Duffing oscillator is characterized by two classical stable solutions with opposite oscillation phase. In the quantum regime, two squeezed states correspond to them. For weak driving, the small-oscillation solution can be identified with the 0-photon quantum state. Since it is favored by photon leaking, it has a low effective temperature and can be regarded as stable in absence of tunneling. However, this stable state is associated to a relative quasienergy maximum, in contrast to the case of a static bistable potential. At a multiphoton resonance, this state becomes metastable and generates a (anti-)resonance of the stationary oscillation. This has been already predicted in Refs. [10, 12, 13], but the link to the semiclassical picture was not drawn. This situation could also occur in a Josephson bifurcation amplifier [17] operating in the quantum regime.

In conclusion, inspired by recent experiments, we have explained the nonlinear response of the driven dissipative Jaynes-Cummings model. We have predicted the existence of a metastable squeezed state in the semiclassical limit and drawn a link between effective local temperature and the squeezing parameter. We have analyzed the escape mechanisms from the metastable states and found resonant dynamical tunneling. Our analysis reveals generic features on the dissipative dynamics of nonlinear driven quantum systems.

We thank M. I. Dykman, M. H. Devoret and V. Leyton for useful discussions and acknowledge support by the Forschungsförderungsfonds of the Universität Düsseldorf, the Excellence Initiative of the German Federal and State Governments, and the DAAD-PROCOL Program.

- 
- [1] E.T. Jaynes and F.W. Cummings, Proc. IEEE **51**, 89 (1963)
  - [2] J. Larson, Phys. Scr. **76**, 146 (2007).
  - [3] A. Wallraff *et al.*, Nature **431**, 162 (2004).
  - [4] I. Chiorescu *et al.*, Nature **431**, 159 (2004).
  - [5] N. Hatakenaka and S. Kurihara, Phys. Rev. A **54**, 1729 (1996).
  - [6] M. Winger *et al.*, Phys. Rev. Lett. **101**, 226808 (2008).
  - [7] L.S. Bishop *et al.*, Nature Phys. **5**, 105 (2009).
  - [8] M.I. Dykman and V.N. Smelyanskii, Sov. Phys. JETP **67**, 1769 (1989).
  - [9] M. Marthaler and M.I. Dykman, Phys. Rev. A **73**, 042108 (2006).
  - [10] V. Peano and M. Thorwart, Phys. Rev. B **70**, 235401 (2004).
  - [11] M.I. Dykman and M.V. Fistul, Phys. Rev. B **71**, 140508(R) (2005).
  - [12] V. Peano and M. Thorwart, Chem. Phys. **322**, 135 (2006).
  - [13] V. Peano and M. Thorwart, New J. Phys. **8**, 21 (2006).
  - [14] A. A. Houck *et al.*, Phys. Rev. Lett. **101**, 080502 (2008).
  - [15] Y.T. Chough, H. Nha, and K. An, J. Phys. Soc. Jpn. **69**, 4060 (2000).
  - [16] H. P. Yuen, Phys. Rev. A **13**, 2226 (1976).
  - [17] I. Siddiqi *et al.*, Phys. Rev. Lett. **93**, 207002 (2004).